Available online at www.sciencedirect.com
SCIENCE DIRECT
Polymer 47 (2006) 1741–1748
polymer
www.elsevier.com/locate/polymer

Modeling of effective elastic properties for polymer based carbon nanotube composites

Young Seok Song, Jae Ryoun Youn *

School of Materials Science and Engineering, Seoul National University, 56-1, Shinlim-Dong, Gwanak-Gu, Seoul 151-744, South Korea

Received 30 September 2005; received in revised form 5 January 2006; accepted 5 January 2006

Abstract

Effective elastic properties of the nanocomposites filled with carbon nanotubes (CNTs) are investigated by the asymptotic expansion homogenization (AEH) method. In order to implement the homogenization method, a control volume finite element method (CVFEM) is employed in contrast to the previous studies. It is assumed that the nanocomposites have geometric periodicity with respect to local length scale and the elastic properties of nanocomposites can be represented by those of the representative volume element (RVE). Random orientation of the CNTs embedded in the nanocomposites is considered by using the orientation tensor. The effective elasticity tensor predicted by the homogenization method is compared with analytical and experimental results. In the experiment, the CNT surface is treated by oxygen plasma to improve interfacial bonding between the CNT and the matrix and to disperse the CNTs homogeneously in epoxy resin because the perfect interfacial bonding is presumed in the homogenization method. Homogeneous CNT dispersion is experimentally identified by the field emission scanning electronic microscope (FESEM). It is found that the numerically calculated elastic modulus is in good agreement with that obtained by analytic model.

Keywords: Carbon nanotubes; Elastic properties; Homogenization method

1. Introduction

Polymeric nanocomposites filled with such nanoparticles as carbon nanotubes, nanoclays, and nanofibers have attracted a large amount of attention to achieve more enhanced mechanical, thermal, and electrical properties than conventional composites [1]. Especially, it has been addressed that the carbon nanotube (CNT) has outstanding Young's modulus and tensile strength and is one of the most promising materials with potential as an ultimate reinforcing material in the nanocomposites [2–4]. Previous studies on the mechanical properties of the CNT show that it has quite broad variation of the Young's modulus ranging from 200 to 4 TPa, tensile strength from 10 to 200 GPa, and bending strength of about 20 GPa [5–8]. The measured and predicted mechanical properties of CNTs are varied depending on the size of the CNT, structure of the CNT, and experimental tools such as atomic force microscope (AFM) or transmission electron microscope (TEM).

Many experimental investigations on mechanical properties of the CNT filled nanocomposites have been carried out but more studies are needed to realize the potential of CNTs as the reinforcement [9–11]. In the case of layered silicate polymer composites, quite a few studies have been performed to obtain the mechanical properties numerically and theoretically and considerable achievements are reported [12–19].

Numerical computation of the material properties including mechanical, thermal, and electrical properties is a challenging task for producing and designing a novel nanocomposite. The computational approach can be divided into two methods, i.e. molecular dynamics (MD) and continuum mechanics based methods. The MD has yielded many simulation results to understand the behavior of individual and bundled CNTs. Either computational power or numerical algorithm for the MD has been improved rapidly. However, the MD is still limited to simulation of a system containing 10^6–10^8 atoms for the period of a few nanoseconds, that is, very small length and time scales. The MD simulation has difficulties in handling nanocomposites with large length and time scales. Therefore, the simulation for larger systems or longer time is currently left to continuum mechanics method. The continuum mechanics based approach which also includes analytic theories such as Halpin–Tsai Eq. [20] or Mori–Tanaka Eq. [21] still needs validation process to

* Corresponding author. Tel.: +82 2 880 8326; fax: +82 2 885 1748.
E-mail address: jaeryoun@snu.ac.kr (J.R. Youn).

0032-3861/$ - see front matter © 2006 Elsevier Ltd. All rights reserved.
doi:10.1016/j.polymer.2006.01.013

get rid of doubts on acceptability but is efficient enough to obtain the mechanical properties of nanocomposites with minimum time and cost.

Studies on numerical calculation of the mechanical properties of the nanocomposites filled with CNTs have been rarely reported [22–25]. Chen and Liu [24,25] evaluated effective mechanical properties of the nanocomposites embedded with the CNT using a representative volume element (RVE) and finite element method (FEM) and provided numerical results accordant with experimental ones.

There are plenty of studies on prediction of physical properties by using the homogenization method for composite materials with periodic microstructure [26–37]. Most of them are carried out to obtain the effective mechanical properties of composites reinforced by continuous fiber structures such as woven fabrics and braided preforms based on the finite element method (FEM) and the boundary element method (BEM) [35,36]. The homogenization method is a powerful tool by which a heterogeneous medium is transformed to the equivalent homogeneous medium with the same internal energy as shown in Fig. 1. The asymptotic expansion homogenization (AEH) method adopted in this study is able to perform both localization and homogenization for the heterogeneous medium. The homogenization method assumes that all the physical quantities vary in both local and global scales and the quantities are periodic with respect to the local scale due to the periodicity of the geometrical microstructure. As the periodic dimension approaches zero, the homogenized effective material properties are obtained and their asymptotic behavior can be calculated. Because of these attractive features, the homogenization method has been widely adopted for predicting elastic properties such as Young's modulus and optimizing the topology of the composite structure [37]. In the general homogenization process, a representative volume element (RVE) is constructed for composites with periodic structure and the scale parameter relating dimension of the RVE to that of the entire composite is employed.

In this study, the effective elasticity tensor of the CNT filled nanocomposite is examined by using the homogenization method. Effects of aspect ratio and concentration of CNTs on the elasticity tensor are investigated. In contrast to most of the previous studies, which used FEM or BEM for the homogenization method, the control volume finite element method (CVFEM) is adopted in this study. In order to compare the numerical results with analytic ones, the analytic model proposed by Halpin and Tsai [20] is employed. The numerically predicted axial tensile modulus is also verified by comparing it with experimental results.

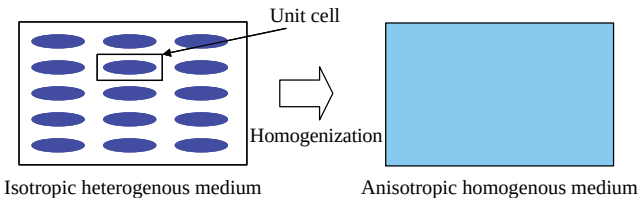

Fig. 1. Schematic illustration of homogenization method.

2. Homogenization method

2.1. Modeling of effective elasticity tensor

Fig. 2 shows a RVE employed in this study, which consists of three different regions, i.e. air, CNT, and matrix. The RVE is constructed based on the following assumptions: (i) the CNTs are homogeneously dispersed in the nanocomposites with the square packing, (ii) they are perfectly bonded with the matrix and have uniform dimensions such as their length, inner, and outer diameters, (iii) there is no direct interaction between the adjacent CNTs, (iv) the CNT nanocomposites contain the periodic unit cell which includes a single CNT aligned unidirectionally. Small amount of CNTs are loaded in the nanocomposites so that the above assumptions should be valid. As shown in Fig. 2, nanocomposites composed of many periodic unit cells have a characteristic length scale, L, in the macroscopic scale and the RVE has a characteristic length, l, in the microscopic scale. An important parameter in

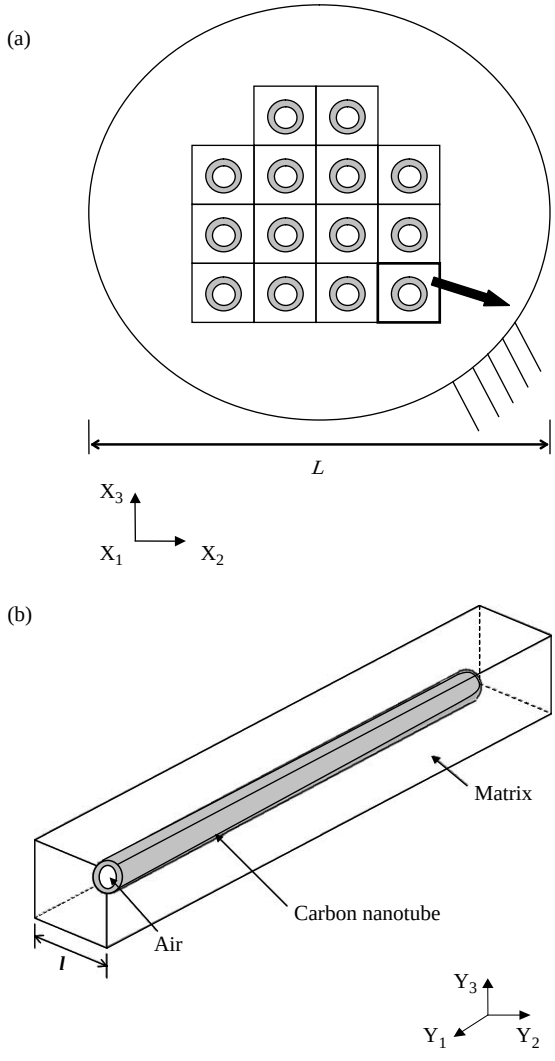

Fig. 2. (a) CNT filled nanocomposties with periodic structure and (b) representative volume element (RVE) with a single carbon nanotube in microscopic scale.

the homogenization process is the ratio of these characteristic lengths, $\omega = l/L$. Since the periodic domain, Ω, is quite small compared with the entire scale for nanocomposites, $\omega \ll 1$. The RVE containing a single CNT is composed of air, CNT, and matrix, whose domains are denoted by Ω_a, Ω_c, and Ω_m, respectively. On the other hand, the air region reduces overall mechanical properties of the RVE because it acts as a void and has no mechanical properties. In the current study, the mechanical properties of the air are not taken into account. It is assumed that the mechanical properties of the CNT and matrix are linearly elastic, isotropic, and homogeneous. As a result, the RVE becomes transversely isotropic with five independent material constants. Two distinct coordinate systems, i.e. macroscopic scale x_i and microscopic scale y_i are adopted in the asymptotic expansion homogenization (AEH) method and they can describe the macroscopic and microscopic behaviors of the CNT filled nanocomposites. The global coordinate system, x_i, is related to the local coordinate system, y_i, as shown below.

$$y_i = \frac{x_i}{\omega} \tag{1}$$

It is assumed that elasticity tensor, C_{ijkl}, of the nanocomposite is periodic with respect to y_i. The elasticity tensor is expressed by using the relationship between macroscopic and microscopic scales as the following.

$$C^{\omega}_{ijkl}(x_i) = C_{ijkl}\left(\frac{x_i}{\omega}\right) = C_{ijkl}(y_i) \tag{2}$$

where C^{ω}_{ijkl} is the periodic function with respect to the microscopic scale. Eq. (2) allows us to define the macroscopic material properties in terms of the microscopic ones.

The linear elastic boundary value problem on the RVE is expressed as follows.

$$\frac{\partial \sigma^{\omega}_{ij}}{\partial x_j} + f_i = 0 \quad \text{in } \Omega \tag{3}$$

$$u^{\omega}_i = 0 \quad \text{on } \partial\Omega \tag{4}$$

$$\sigma^{\omega}_{ij} n_j = F_i \quad \text{on } \partial\Omega \tag{5}$$

$$\varepsilon_{ij}\left(u^{\omega}_i\right) = \frac{1}{2}\left(\frac{\partial u^{\omega}_i}{\partial x_j} + \frac{\partial u^{\omega}_j}{\partial x_i}\right) \tag{6}$$

$$\sigma^{\omega}_{ij} = C^{\omega}_{ijkl}\varepsilon_{kl}\left(u^{\omega}_i\right) \tag{7}$$

where $\partial\Omega$ represents the boundary region and superscript, ω, indicates the real material behavior. σ_{ij}, ε_{ij}, and u_i are the stress tensor, strain tensor, and displacement vector, respectively. In the homogenization process, all of the physical properties are assumed to be periodic with respect to the local scales, which allows us to decouple the global and the local scales by using a perturbation technique [38]. Multi-scale asymptotic expansions for the displacement is given as the following.

$$u^{\omega}_i(x_i) = u^{(0)}_i(x_i,y_i) + \omega u^{(1)}_i(x_i,y_i) + \omega^2 u^{(2)}_i(x_i,y_i) + \ldots \tag{8}$$

where it is assumed that $u^{\omega}_i(x_i,y_i)$ is periodic in local coordinate system, y_i. From the chain rule, differential operator is expressed as

$$\frac{\partial}{\partial x_i} = \frac{\partial}{\partial x_i} + \frac{1}{\omega}\frac{\partial}{\partial y_i} \tag{9}$$

By substituting Eq. (9) into Eq. (6), the strain tensor is rewritten as below.

$$\varepsilon_{ij} = \frac{1}{\omega}\varepsilon^{-1}_{ij}(x_i,y_i) + \varepsilon^{0}_{ij}(x_i,y_i) + \omega\varepsilon^{1}_{ij}(x_i,y_i) + \ldots \tag{10}$$

where

$$\varepsilon^{-1}_{ij}(x_i,y_i) = \frac{1}{2}\left(\frac{\partial u^{(0)}}{\partial y_j} + \frac{\partial u^{(0)}}{\partial y_i}\right) \tag{11}$$

$$\varepsilon^{0}_{ij}(x_i,y_i) = \frac{1}{2}\left(\frac{\partial u^{(0)}}{\partial x_j} + \frac{\partial u^{(0)}}{\partial x_i}\right) + \frac{1}{2}\left(\frac{\partial u^{(1)}}{\partial y_j} + \frac{\partial u^{(1)}}{\partial y_i}\right) \tag{12}$$

$$\varepsilon^{1}_{ij}(x_i,y_i) = \frac{1}{2}\left(\frac{\partial u^{(1)}}{\partial x_j} + \frac{\partial u^{(1)}}{\partial x_i}\right) + \frac{1}{2}\left(\frac{\partial u^{(2)}}{\partial y_j} + \frac{\partial u^{(2)}}{\partial y_i}\right) \tag{13}$$

Combination of Eqs. (3) and (7) yields the following equation.

$$\frac{\partial}{\partial x_j}\left[C_{ijkl}\left(\frac{x_i}{\omega}\right)\varepsilon_{kl}\left(u^{\omega}_i\right)\right] + f_i = 0 \tag{14}$$

After substitution of the above strain tensor equations into Eq. (14), The following three hierarchical equations are obtained by arranging the terms with the same order of ω.

$$\frac{\partial}{\partial y_j}\left[C_{ijkl}\frac{\partial u^{(0)}_k}{\partial y_l}\right] = 0 \tag{15}$$

$$\frac{\partial}{\partial x_j}\left[C_{ijkl}\frac{\partial u^{(0)}_k}{\partial y_l}\right] + \frac{\partial}{\partial y_j}\left[C_{ijkl}\left(\frac{\partial u^{(0)}_k}{\partial x_l} + \frac{\partial u^{(1)}_k}{\partial y_l}\right)\right] = 0 \tag{16}$$

$$\frac{\partial}{\partial x_j}\left[C_{ijkl}\left(\frac{\partial u^{(0)}_k}{\partial x_l} + \frac{\partial u^{(1)}_k}{\partial y_l}\right)\right] + \frac{\partial}{\partial y_j}\left[C_{ijkl}\left(\frac{\partial u^{(1)}_k}{\partial x_l} + \frac{\partial u^{(2)}_k}{\partial y_l}\right)\right] = 0 \tag{17}$$

In the homogenization process, the terms with same order of ω should be zero to ensure that the asymptotic series approximation is valid as ω approaches zero. From Eq. (15), it is assumed that $u^{(0)}_k$ is independent of the local coordinate system, y_i.

$$u^{(0)}_i(x_i,y_i) = u^{(0)}_i(x_i) \tag{18}$$

Consequently, the so-called micro-equation (16) takes the following form.

$$\frac{\partial}{\partial y_j}\left[C_{ijkl}\left(\frac{\partial u^{(0)}_k}{\partial x_l} + \frac{\partial u^{(1)}_k}{\partial y_l}\right)\right] = 0 \tag{19}$$

Now that the current problem has the linearity, the perturbation term, $u^{(1)}_k$, is given through separation of x_i

from y_i as below

$$u_i^{(1)}(x_i,y_i) = -\chi_i^{kl}(y_i)\frac{\partial u_k^{(0)}(x_i)}{\partial x_l} + u_i^{(1)}(x_i) \tag{20}$$

where χ_i^{kl} is the arbitrary characteristic function with periodicity with respect to y_i. By substituting Eq. (20) into Eq. (19), the governing equation is obtained as the following.

$$\frac{\partial}{\partial y_j}\left(C_{ijmn}(y_i)\frac{\partial \chi_m^{kl}(y_i)}{\partial y_n}\right) - \frac{\partial}{\partial y_j}C_{ijkl}(y_i) = 0 \tag{21}$$

As the strain tensor is approximated in a power series of ω, the stress tensor can be expanded asymptotically as follows.

$$\sigma_{ij}^{\omega} = \frac{1}{\omega}\sigma_{ij}^{-1}(x_i,y_i) + \sigma_{ij}^{0}(x_i,y_i) + \omega\sigma_{ij}^{1}(x_i,y_i) + \ldots \tag{22}$$

where

$$\sigma_{ij}^{0} = C_{ijkl}^{\omega}\left(\frac{\partial u_k^{(0)}}{\partial x_l} + \frac{\partial u_k^{(1)}}{\partial y_l}\right) \tag{23}$$

By substituting Eq. (20) into Eq. (23), the following equation is obtained.

$$\sigma_{ij}^{0} = \left(C_{ijkl} - C_{ijmn}\frac{\partial \chi_m^{kl}}{\partial y_n}\right)\frac{\partial u_k^{(0)}}{\partial x_l} \tag{24}$$

The effective elasticity tensor, $\tilde{C}_{ijkl}$, is cast as follows by using the relationship between the homogenized stress and the displacement gradient tensor.

$$\tilde{\sigma}_{ij}^{0} = \tilde{C}_{ijkl}\frac{\partial u_k^{(0)}}{\partial x_l} \tag{25}$$

where

$$\tilde{\sigma}_{ij}^{0} = \frac{1}{\Omega}\int_{\Omega}\sigma_{ij}^{0}\mathrm{d}y \tag{26}$$

$$\tilde{C}_{ijkl} = \frac{1}{\Omega}\int_{\Omega}\left(C_{ijkl} - C_{ijmn}\frac{\partial \chi_m^{kl}}{\partial y_n}\right)\mathrm{d}y \tag{27}$$

C_{ijkl} has different values for each region of the RVE and the above integration is taken over the entire RVE domain.

2.2. Numerical method

The control volume finite element method (CVFEM) used in the previous study [39] is adopted to solve a set of the coupled partial differential equations formed by the governing Eq. (21). In general, the CVFEM has been applied to heat transfer and fluid flow problems and has produced encouraging results compared with the conventional finite element method (FEM). Since the Eq. (21) has elliptical characteristics, the CVFEM is chosen as a numerical method. Eq. (21) is expressed in the general form as the following.

$$\frac{\partial J_j}{\partial y_j} = S \tag{28}$$

where J_i is the diffusion flux and S is the source term. These are given by

$$J_j = C_{ijmn}\frac{\partial \chi_m^{kl}}{\partial y_n} - C_{ijkl} \tag{29}$$

$$S = 0 \tag{30}$$

Because the CVFEM is based on the conservation principle within control volume, we integrate Eq. (28) over the control volume as the following.

$$\int_{\partial V} J_i n_i \mathrm{d}s = \int_{\partial V} S\mathrm{d}V \tag{31}$$

where ∂V is the control surface and n_i is the outward unit vector normal to the differential area, ds. Details of the numerical method used in the present study are described in the previous investigation [39].

Mechanical properties of the matrix and the CNT obtained from experiments and literature [5–8] and dimension of the RVE are listed in Table 1. In order to investigate the effect of the aspect ratio, sizes of the RVE and CNT are not kept constant. Based on the convergence test of finite element mesh, 124,576 elements and 602,423 nodes are used in the calculation. The periodic boundary conditions are imposed on the walls of the RVE. It is assumed that the RVE, which contains an aligned single CNT has transversely isotropic properties. However, since the CNTs are randomly dispersed in the nanocomposites, it is necessary to consider orientation of the CNTs in order to predict material properties of the real CNT nanocomposites. Therefore, by using orientation averaging which has been utilized in short fiber reinforced composites, the effective mechanical properties for nanocomposites filled with randomly dispersed CNTs are obtained. The second order orientation tensor proposed by Tucker and Advani [39] is adopted for describing the orientation state of CNTs because the tensor representation is compact enough to handle the overall orientation distribution of the CNTs more practically than the distribution function, ψ. The orientation tensor is defined as the following.

$$a_{ij} = \oint p_i p_j \psi(\boldsymbol{p})\mathrm{d}\boldsymbol{p} \tag{32}$$

Table 1
Properties of matrix and CNT and dimension of the RVE used in the homogenization process

	Matrix	CNT
Young's modulus (GPa)	1.21	270
Shear modulus (GPa)	0.48	107
Poisson's ratio	0.35	0.3
Dimension	Height: 151 nm	Outer diameter: 13 nm
	Width: 151 nm	Inner diameter: 4 nm

where $\boldsymbol{p}$ is the unit vector in the axial direction of CNT and $\psi(\boldsymbol{p})$ is the orientation distribution function.

It is presumed that the CNT and the matrix show linear elastic behavior and magnitude of the applied stress does not lead to debonding or cracking. The real nanocomposite is regarded as an assembly of all the RVE's, which experience the same strain regardless of their orientation. The bounding approach for the elasticity tensor of the nanocomposite, which is the simple average of the RVE's over all the directions, is expressed below.

$$\langle C_{ijkl}\rangle = \oint C_{ijkl}(\boldsymbol{p})\psi(\boldsymbol{p})\mathrm{d}\boldsymbol{p} \tag{33}$$

The bulk stress–strain relationship of the nanocomposite is written in terms of the generalized Hooke's law.

$$\sigma_{ij} = \langle C_{ijkl}\rangle \varepsilon_{kl} \tag{34}$$

The orientation averaging approach is based on the assumption that the single RVE can stand for the structure of real nanocomposites. Eq. (33) is denoted by orientation tensors as below.

$$\begin{aligned}\langle C_{ijkl}\rangle = {} & B_1(a_{ijkl}) + B_2(a_{ij}\delta_{kl} + a_{kl}\delta_{ij}) + B_3(a_{ik}\delta_{jl} \\ & + a_{il}\delta_{jk} + a_{jl}\delta_{ik} + a_{jk}\delta_{il}) + B_4(\delta_{ij}\delta_{kl}) \\ & + B_5(\delta_{ik}\delta_{jl} + \delta_{il}\delta_{jk})\end{aligned} \tag{35}$$

The averaged elasticity tensor has 21 independent components and is expressed in terms of the second and fourth order orientation tensors. Five constants from B_1 to B_5 are the invariants, which are calculated from the transversely isotropic properties of the RVE [40]. Since Eq. (35) contains a fourth order orientation tensor, approximation of the fourth order orientation tensor by the second order orientation tensor is needed. In the present study, we take two cases into account; unidirectional and random orientation of CNTs. It is known that the hybrid closure approximation proposed by Advani and Tucker [41] describes the random and unidirectional orientation states of short fibers properly. In the case of random orientation, the closure approximation becomes as follows.

$$\begin{aligned}a_{ijkl} = {} & -\frac{1}{35}(\delta_{ij}\delta_{kl} + \delta_{ik}\delta_{jl} + \delta_{il}\delta_{jk}) + \frac{1}{7}(a_{ij}\delta_{kl} + a_{ik}\delta_{jl} \\ & + a_{il}\delta_{jk} + a_{kl}\delta_{ij} + a_{jl}\delta_{ik} + a_{jk}\delta_{il})\end{aligned} \tag{36}$$

2.3. Analytic model

It is assumed that the RVE shown in Fig. 2(b) includes a single CNT surrounded by the matrix of the same volume fraction as that in the entire nanocomposite and is transversely isotropic. For the validation of numerically homogenized elastic properties, the following analytic equation suggested by Halpin and Tsai [20] is employed.

$$\frac{M}{M_\mathrm{m}} = \frac{1 + \varsigma\tilde{\xi}\phi_\mathrm{c}}{1 - \tilde{\xi}\phi_\mathrm{c}} \tag{37}$$

$$\tilde{\xi} = \frac{(M_\mathrm{c}/M_\mathrm{m}) - 1}{(M_\mathrm{c}/M_\mathrm{m}) + \varsigma} \tag{38}$$

where M represents the axial modulus (E_1), the transverse modulus (E_2), the in-plane shear modulus (G_{12}) or the out-of-plane shear modulus (G_{23}). Subscripts c and m denote the CNT and the matrix, respectively. ϕ_c is the volume fraction of CNTs. ς is defined as follows.

$$\varsigma_{E_1} = 2\frac{L}{D} \tag{39}$$

$$\varsigma_{E_2} = 2 \tag{40}$$

$$\varsigma_{G_{12}} = 1 \tag{41}$$

$$\varsigma_{G_{23}} = \frac{K_\mathrm{m}/G_\mathrm{m}}{K_\mathrm{m}/G_\mathrm{m} + 2} \tag{42}$$

where L and D are the length and the outer diameter of CNT. Because the analytic model is proposed for application to the composites filled with rod-shaped particles such as short fibers, it has some limitations to shells or hollow structures. Poisson's ratio can be obtained by the rule of mixture as below.

$$\nu_{12} = \nu_\mathrm{f}\phi_\mathrm{f} + \nu_\mathrm{m}(1 - \phi_\mathrm{m}) \tag{43}$$

ν_{21} and ν_{23} are given from consideration of symmetry constraints as follows.

$$\nu_{21} = \nu_{12}\frac{E_2}{E_1} \tag{44}$$

$$\nu_{23} = \frac{E_2}{2G_{23}} - 1 \tag{45}$$

where the axial direction of CNT is considered as one-direction in Cartesian coordinate system. The elastic constants obtained by the above equations have the following relationship with the elasticity tensor components of the RVE.

$$C_{1111} = \frac{(1 - \nu_{23})E_1}{1 - \nu_{23} - 2\nu_{12}\nu_{21}} \tag{46}$$

$$C_{2222} = \frac{E_2}{2(1 - \nu_{23} - 2\nu_{12}\nu_{21})} + G_{23} \tag{47}$$

$$C_{1122} = \frac{\nu_{21}E_1}{1 - \nu_{23} - 2\nu_{12}\nu_{21}} \tag{48}$$

$$C_{2233} = \frac{E_2}{2(1 - \nu_{23} - 2\nu_{12}\nu_{21})} - G_{23} \tag{49}$$

$$C_{1212} = G_{12} \tag{50}$$

3. Experimental

It has been reported that chemical functionalization or surface modification of CNTs improves dispersion of the CNT and the strength of interfacial bonding between the CNTs and

the polymer matrix [42]. Therefore, in order to obtain good and homogeneous dispersion of the CNTs in the epoxy resin, acid treatment for the CNTs was carried out, which could get rid of impurities including amorphous carbons, graphite particles, and metal catalysts. After the CNTs were treated in a 3:1 mixture of 65% H_2SO_4/HNO_3 at 100 °C for 30 min, the treated CNTs were washed with distilled water and then dried in a vacuum oven for a day. The acid treatment is known to introduce hydroxylic functional groups to the surface of CNTs. Multiwalled carbon nanotubes synthesized by chemical vapor deposition (CVD) and an epoxy resin were employed. Details of the preparation process of the specimen were described in the previous studies [9]. Plasma surface treatment of the CNT was carried out to improve the interfacial bonding between the CNTs and the matrix. The surface modification was performed by using Ar plasma with 1% O_2 and the plasma power was 200 W. The nanocomposites filled with CNTs of 0.5 and 1.0% volume fraction (0.29 and 0.58% volume fraction, respectively) were prepared and mechanical tests were conducted to obtain mechanical properties by using Instron 5548. For averaging of the data, at least five samples were prepared at each CNT weight fraction. The tensile experiments were performed at ambient temperature and at the constant crosshead speed of 2 mm/min. In order to identify the surface elemental composition, X-ray photoelectron spectroscopy (XPS) was utilized. From shifting of main peak, the existence of oxygen bonding to the CNT was verified. The CNT dispersion was morphologically characterized through a FESEM (JEOL JSM-6330F).

4. Results and discussion

Plasma surface treatment is carried out in order to enhance the interfacial bonding between the CNTs and the matrix because perfect interfacial bonding between the CNTs and the matrix is assumed in the homogenization. Fig. 3 represents that the CNTs are dispersed in the matrix homogeneously. It is shown by the FESEM image that the CNTs are not pulled out

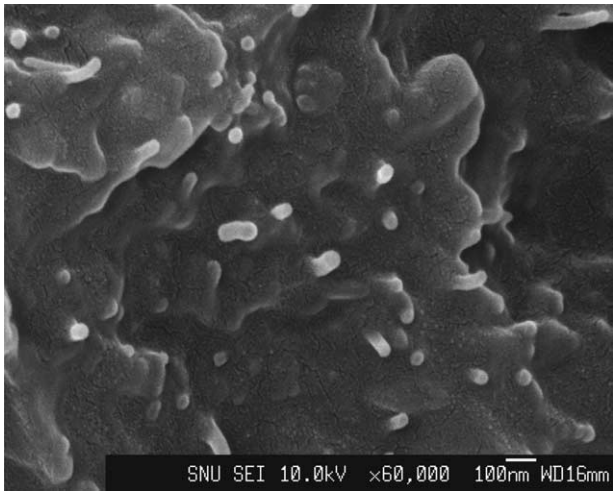

Fig. 3. FESEM image of the nanocomposites filled with carbon nanotubes.

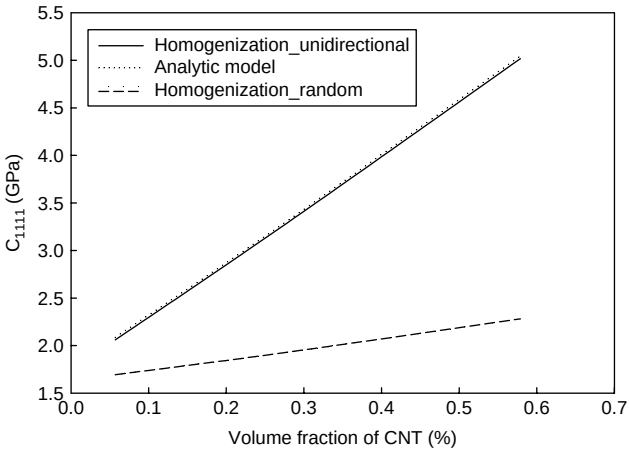

Fig. 4. C_{1111} calculated analytically and numerically with respect to the CNT volume fraction.

but broken due to the strong interfacial bonding between the CNTs and the epoxy resin when tensile force is imposed. It is believed that the oxygen group generated on the CNT surface by the plasma treatment causes good dispersion and strong interfacial bonding. Eq. (34), the generalized Hook's law, can be rewritten in the following contracted notation form [43].

$$\sigma_i = C_{ij}\varepsilon_j \quad i,j = 1,\ldots,6 \tag{51}$$

When the CNTs are added in the epoxy resin, the homogenized elasticity tensor calculated for a RVE is given by the following stiffness matrix.

$$C_{ij} = \begin{bmatrix} 5.02 & 0.64 & 0.64 & 0 & 0 & 0 \\ 0.64 & 1.60 & 0.43 & 0 & 0 & 0 \\ 0.64 & 0.43 & 1.60 & 0 & 0 & 0 \\ 0 & 0 & 0 & 0.58 & 0 & 0 \\ 0 & 0 & 0 & 0 & 0.48 & 0 \\ 0 & 0 & 0 & 0 & 0 & 0.48 \end{bmatrix} \text{GPa} \tag{52}$$

The elasticity tensor represents large anisotropy for elastic properties of the RVE.

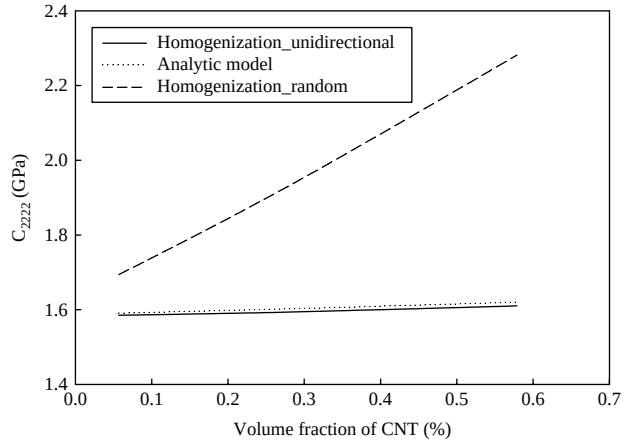

Fig. 5. C_{2222} calculated analytically and numerically with respect to the CNT volume fraction.

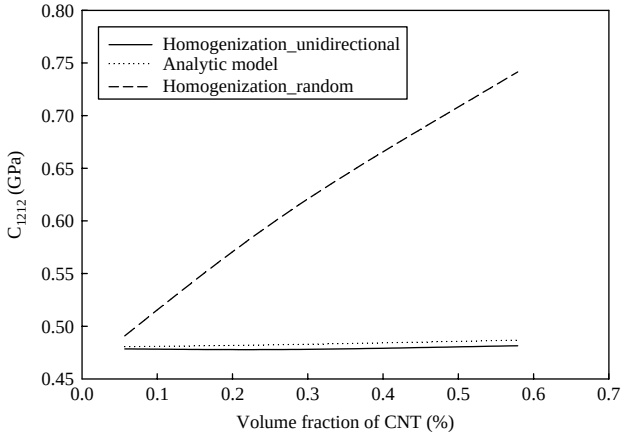

Fig. 6. C_{1212} calculated analytically and numerically with respect to the CNT volume fraction.

Fig. 4 shows C_{1111} component of the effective elasticity tensor obtained by the homogenization technique and Halpin–Tsai equation. When the CNTs are aligned unidirectionally in the nanocomposite, the homogenization method exhibits the same prediction as the analytic model. On the other hand, in the case that the CNTs are randomly oriented, the averaged C_{1111} obtained by using orientation tensor is quite lower than that calculated for the RVE. As shown in Fig. 4, the C_{1111} component is linearly increased with respect to the CNT volume fraction because small volume fraction of the CNT is considered in this study. The C_{2222} component of the effective elasticity tensor is represented in Fig. 5. The results obtained analytically are slightly higher than those calculated numerically for the nanocomposites filled with unidirectionally dispersed CNTs. In contrast to the C_{1111}, the C_{2222} obtained for random orientation of CNTs is much higher than that calculated for the RVE containing an axially oriented CNT. Fig. 6 shows variation of the C_{1212} component as a function of CNT volume fraction. It is found that the shear modulus is nearly independent of the CNT volume fraction for the nanocomposites embedded with unidirectionally aligned CNTs. The Halpin–Tsai equation provides a good approximation because the equation is a semi-empirical function.

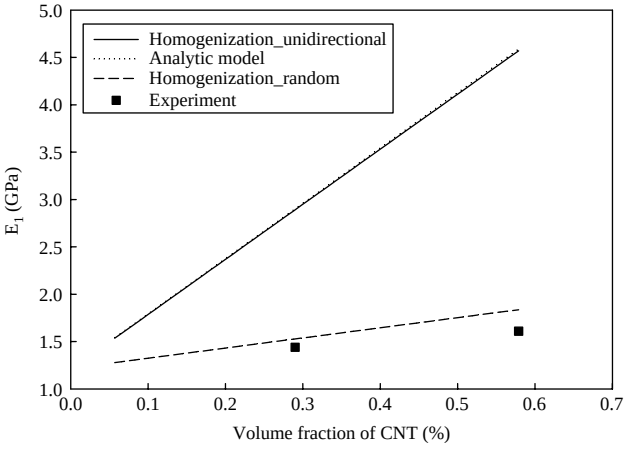

Fig. 7. Axial tensile moduli predicted with respect to the CNT volume fraction.

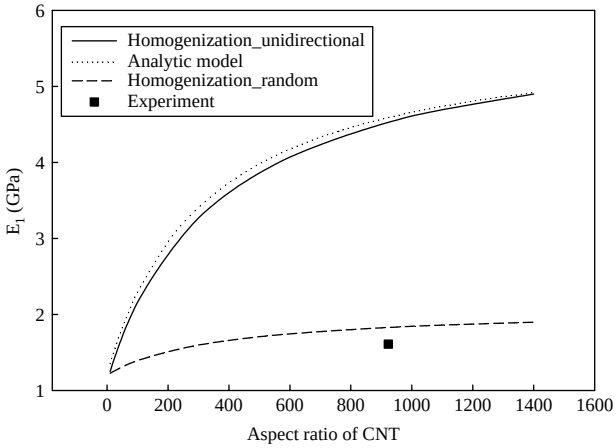

Fig. 8. Axial tensile moduli predicted with respect to the aspect ratio of CNT.

In order to validate the results calculated by the homogenization method, experimental results are compared with them as shown in Fig. 7. The measured axial tensile modulus is somewhat different from that predicted by the homogenization method. The discrepancy is attributed to the following two reasons. One is that all of the CNTs are assumed to be straight in the nanocomposites, although waviness of the CNT affects mechanical properties of the nanocomposites. The other reason is that accurate material properties of CNTs are not used as input parameters in the homogenization process. There are limitations and difficulties in measuring exact material data of the CNTs used in the nanocomposites. In order to investigate the effect of the aspect ratio of CNT on the axial modulus, length of the CNT in the RVE is altered. As shown in Fig. 8, the axial tensile modulus is varied with respect to the aspect ratio of CNT. The analytically obtained modulus is higher than the homogenized modulus and both of them approach a limiting value gradually, i.e. the modulus obtained by the rule of mixture is increased with respect to the aspect ratio. Findings from comparison between numerical and experimental results indicate that the bounding approach by the orientation tensor is an efficient method considering the contribution of the randomly oriented CNTs in the nanocomposites.

5. Conclusions

Modeling of elastic properties of the nanocomposies embedded with CNTs is carried out by using the homogenization technique. Assuming that the CNT/epoxy nanocomposites have geometrical periodicity with respect to microscopic scale, a representative volume element (RVE) is constructed for the asymptotic expansion homogenization (AEH) method. The control volume finite element method (CVFEM) is adopted in order to implement the homogenization method unlike the previous studies. The epoxy nanocomposites filled with plasma treated CNTs are prepared to enhance the interfacial bonding between the CNTs and the matrix and mechanical measurements are carried out to obtain axial tensile modulus of the nanocomposites. The effective elasticity tensor

predicted by the homogenization method is compared with analytical and experimental results. The bounding approach using the orientation tensor is adopted to consider orientation state of the CNTs. It is observed that the homogenized elasticity tensor is in good agreement with the results obtained from Halpin–Tsai equation and is linearly increased with respect to the CNT volume fraction. As the aspect ratio of CNT is increased, the homogenization technique provides higher axial tensile modulus than the analytic model and the moduli obtained by both methods approach the upper limiting value obtained by the rule of mixture. In the homogenization process, material properties used as input parameters are critical to calculate the exact physical properties of the heterogeneous medium. The homogenization method possesses a large potential for the prediction of such physical properties as elastic modulus and thermal conductivity of heterogeneous composite materials because the method can handle the geometrical complexity and material anisotropy properly.

Acknowledgements

This study was supported by the Applied Rheology Center (ARC) which is an Engineering Research Center created by the Korea Science and Engineering Foundation (KOSEF). The authors are grateful for the support.

References

[1] Song YS, Youn JR. Korea-Aust Rheol J 2004;16(4):201–12.
[2] Bhushan B. Springer handbook of nano-technology. New York: Springer; 2004.
[3] Thostenson ET, Ren Z, Chou TW. Compos Sci Technol 2001;61: 1899–912.
[4] Lau KT, Hui D. Composites, Part B 2002;33:263–77.
[5] Yu MF, Lourie O, Dyer MJ, Moloni K, Kelly TF, Ruoff RS. Science 2000; 287:637–40.
[6] Wagner HD, Lourie O, Feldman Y, Tenne R. Appl Phys Lett 1998;72(2): 188–90.
[7] Li F, Cheng HM, Bai S, Su G. Appl Phys Lett 2000;77(20):3161–3.
[8] Lau KT, Chipara M, Ling HY, Hui D. Composites, Part B 2004;35: 95–101.
[9] Song YS, Youn JR. Carbon 2005;43:1378–85.
[10] Schadler LS, Giannaris SC, Ajayan PM. Appl Phys Lett 1998;73(26): 3842–4.
[11] Allaoui A, Bai S, Cheng HM, Bai JB. Compos Sci Technol 2002;62: 1993–8.
[12] Brune DA, Bicerano J. Polymer 2002;43:369–87.
[13] Luo JJ, Daniel IM. Compos Sci Technol 2003;63:1607–16.
[14] Fornes TD, Paul DR. Polymer 2003;44:4993–5013.
[15] Sheng N, Boyce MC, Parks MD, Rutlege GC, Abes JI, Cohen RE. Polymer 2004;45:487–506.
[16] Wang J, Pyrz R. Compos Sci Technol 2004;64:925–34.
[17] Wu YP, Jia QX, Yu DS, Zhang LQ. Polym Test 2004;23:903–9.
[18] Odegard GM, Clancy TC, Gates TS. Polymer 2005;46:553–62.
[19] Minisini B, Tsobnang F. Composites, Part A 2005;36:531–7.
[20] Halpin JC, Kardos JL. Polym Eng Sci 1976;16:344–52.
[21] Mori T, Tanaka K. Acta Metall 1973;21:571–4.
[22] Thostenson ET, Chou TW. J Phys D: Appl Phys 2003;36:573–82.
[23] Haque A, Ramasetty A. Compos Struct 2005;71(1):68–77.
[24] Liu YJ, Chen XL. Mech Mater 2003;35:69–81.
[25] Chen XL, Liu YJ. Comput Mater Sci 2004;29:1–11.
[26] Terada K, Ito T, Kikuchi N. Comput Methods Appl Eng 1998;153: 223–57.
[27] Gibiansky LV, Sigmund O. J Mech Phys Solids 2000;48:461–98.
[28] Kanit T, Forest S, Galliet I, Mounoury V, Jeulin D. Int J Solids Struct 2003;40:3647–79.
[29] Cluni F, Gusella V. Int J Solids Struct 2004;41:1911–23.
[30] Peng X, Cao J. Composites, Part B 2002;33:45–56.
[31] Chung PW, Tamma KK, Namburu RR. Composites, Part A 2001;32: 1291–301.
[32] Yang QS, Becker W. Comput Mater Sci 2004;31:169–80.
[33] Pagano NJ, Yuan FG. Compos Sci Technol 2000;60:2471–88.
[34] Carvelli V, Poggi C. Composites, Part A 2001;32:1425–32.
[35] Kamiński M. Eng Anal Bound Elem 1999;23:815–23.
[36] Okada H, Fukui Y, Kumazawa N. Comput Struct 2001;79:1987–2007.
[37] Sigmund O. J Mech Phys Solids 2000;48:397–428.
[38] Kleiber M, Tran DH. The stochastic finite element method: basic perturbation technique and computer implementation. New York: Wiley; 1992.
[39] Song YS, Chung K, Kang TJ, Youn JR. Compos Sci Technol 2004;64: 1629–36.
[40] Advani SG, Tucker III CL. J Rheol 1987;31(8):751–84.
[41] Advani SG, Tucker III CL. J Rheol 1990;34:367–86.
[42] Lin Y, Rao AM, Sadanadan B, Kenik EA, Sun YP. J Phys Chem B 2002; 106:1294–8.
[43] Jones RM. Mechanics of composite materials. Washington: Scripta Book Company; 1975.